METHYL TRANSFER REACTIONS
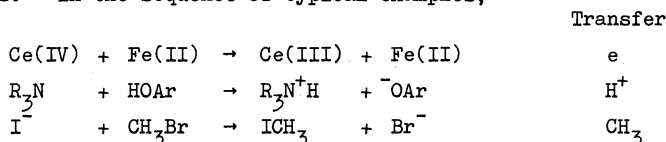

W. John Albery

Department of Chemistry, Imperial College of Science and Technology,
London SW7 2AY


Abstract - The Marcus theory is applied to the transfer of the methyl group
in S_N2 reactions.   Data from 28 reactions are shown to obey the theory.
The symmetry of the transition state for these reactions can then be
deduced.   The use of charge development, the solvent isotope effect, the
α deuterium isotope effect and Hammett relations to locate the transition
state are also discussed.   The information from the various probes is
reconciled and the tightness, as well as the symmetry, of each transition
state is found.

INTRODUCTION

The Marcus theory (1)(2) has been successful in explaining data for electron transfers (3) and
proton transfers (4)(5).   In this paper we show that the theory can be applied to methyl
transfers.   In the sequence of typical examples,

$$\text{Transfer}$$

$$
\begin{array}{lll}
\text{Ce(IV)} + \text{Fe(II)} \rightarrow \text{Ce(III)} + \text{Fe(II)} & \quad \text{e} \\
R_3N + \text{HOAr} \rightarrow R_3N^+H + {}^-\text{OAr} & \quad H^+ \\
I^- + CH_3Br \rightarrow ICH_3 + Br^- & \quad CH_3
\end{array}
$$

we see that the nucleophile and leaving group are analogous to the bases in the proton trans-
fer or the inorganic ions in the electron transfer.   In analysing S_N2 reactions in this
fashion the distinction between the nucleophile and the leaving group becomes blurred;   the
Marcus theory emphasises the symmetry of the reaction.   Particularly important are the para-
meters for the degenerate reaction where the nucleophile and the leaving group are identical,
e.g.

$$Br^- + CH_3Br \rightarrow CH_3Br + Br^-.$$
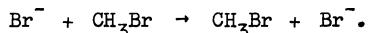
Besides applying the Marcus theory we are also interested in locating the transition state.
This is done most conveniently using two dimensions to represent the geometry or symmetry
of the transition state and the third dimension (plotted as contours) to represent energy or
free energy.   Such diagrams have been used to discuss proton transfers (6), elimination
reactions (7) and acid and base catalysis (8).   Figure 1 shows the diagram for a general
nucleophilic displacement reaction:-

$$X + CY \rightarrow XC + Y$$

The zigzag discontinuities mark association or dissociation steps.   The free energy change
across such discontinuities will depend upon the choice of the standard state and the kinetics
of the association reaction will be second order.   The route through the top right hand
corner is the S_N1 route but since we are concerned with methyl transfers it need concern us
no longer.   The route through the bottom left hand corner is the S_N2 mechanism and we shall
be concerned with the location of the transition state in the bottom left hand corner.   Note
that for a solvolysis reaction there is no preliminary association step and the reaction
starts from (X,CY).   For attack by a solute nucleophile, X, there can be no merging of the
S_N1 and S_N2 transition states (9);   they are on different fragments of Fig.1.   However for
solvolysis reactions there can be a gradual shift from the S_N2 transition state shown to an
S_N1 transition state near (X,C^+,Y).

It is convenient to describe the location of the transition state in terms of the bond orders
for the attacking nucleophile X (η_x) and for the leaving group Y (η_y).   From the Marcus
analysis we obtain values of α which describes the 'symmetry' of the transition state or how
much it resembles the products or reactants.   Figure 2 shows how α varies with η_x and η_y.
We also need to describe the tightness or looseness of the S_N2 transition state and so we
introduce the parameter τ displayed in Fig.3.   In this paper we will use the following probes
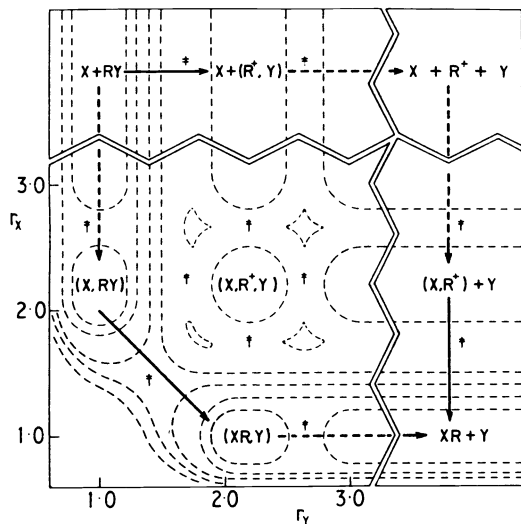to try and place the transition state on the map:-

Fig.1. Schematic free energy surface for the nucleophilic displacement
reaction $X + RY \rightarrow XR + Y$.   The S_N2 route passes through the bottom left hand
corner and the S_N1 route through the top right hand corner.   The zigzag
lines occur where there are steps involving association or dissociation.
The relative heights of the fragments will depend on the choice of the
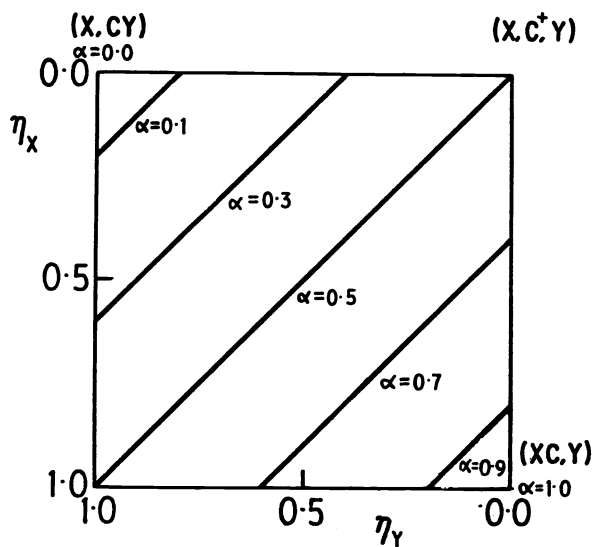standard state.

Fig.2. Contour diagram showing the variation of α, the symmetry parameter,
       with the bond orders of the transition state.

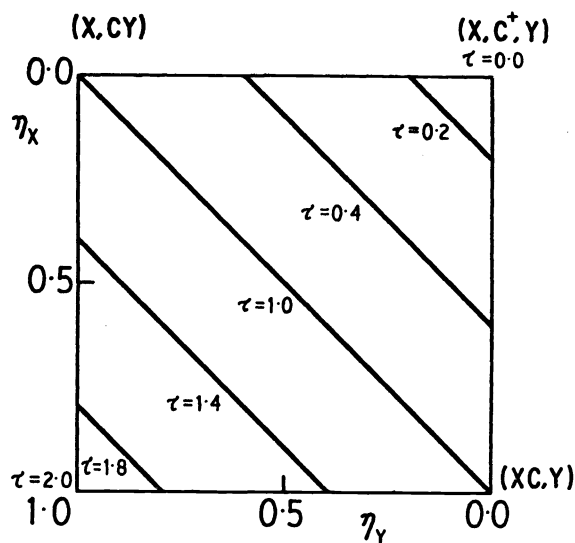| Marcus analysis	α
Charge development	η_Y
Solvent isotope effect	η_X
α D isotope effect	τ
Hammett plots	τ

Fig.3. Contour diagram showing the variation of τ, the tightness parameter, with the bond orders of the transition state.

MARCUS THEORY

For electron transfers the final transfer of the electron takes place in 10^{-16}s and has to be iso-energetic. The free energy of activation then arises from achieving the necessary conditions for the iso-energetic process. This is shown schematically in Fig.4 for a degenerate reaction and in Fig.5 for a downhill reaction. The energy level of the electron is modified by alteration of the surrounding solvent and ligands depicted by the squares, circles and diamonds (10). The Marcus theory assumes that the variation of energy with displacement is parabolic. This arises firstly because small displacements from an equilibrium poisiton normally have a parabolic dependence. Secondly if one sums together many such displacements the lowest energy route on the multi-dimensional surface will still have a parabolic shape. This important result is illustrated in Fig.6 for two such displacements in converting Q to P. The last route, ABC, on the intersecting parabolic bowls is still
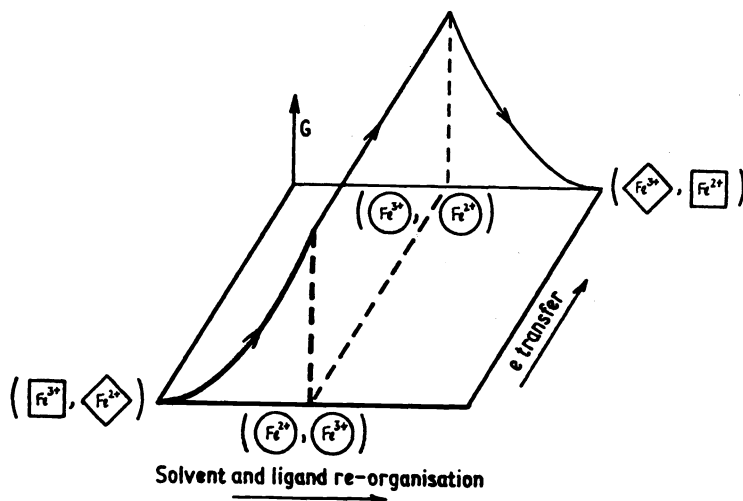

Fig.4. Schematic variation of free energy in a degenerate electron transfer reaction. The changes in solution are indicated by the squares, diamonds and circles.
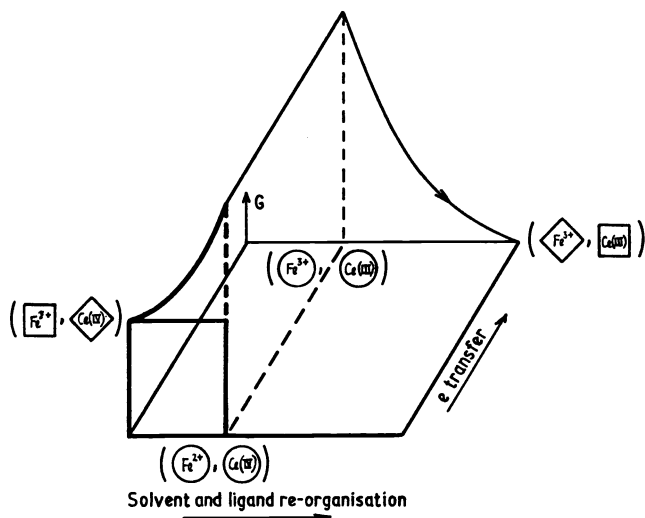
Fig.5. Schematic variation of free energy for an unsymmetrical electron transfer. Note that in the downhill direction the transition state is reactant-like ($\alpha < \frac{1}{2}$) while in the reverse direction it is product-like.
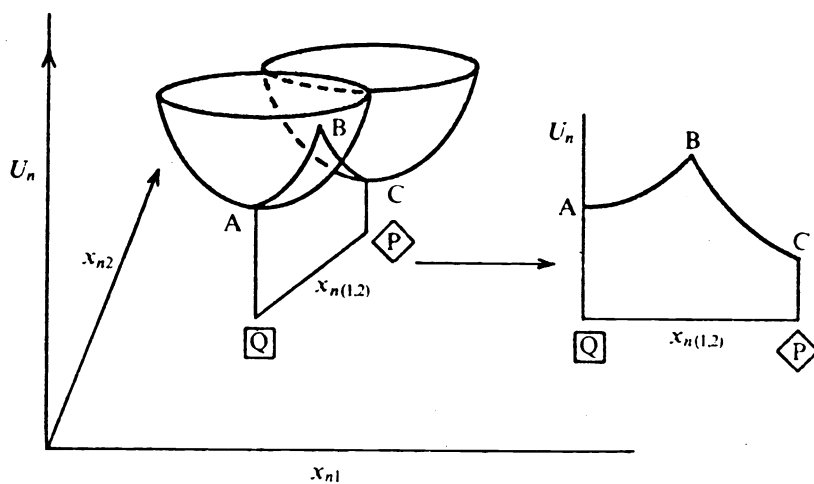

Fig.6. Schematic variation of free energy for converting Q to P when two co-ordinates have to be changed. The intersection of the parabolic bowls still gives the same shape as the barriers in Figs. 4 or 5.

parabolic. The argument can be extended to as many displacements as one wishes.

Although the final electron transfer is iso-energetic this will not be true for the transfer of heavier entities such as the proton or a methyl group. In these cases the profile on the transfer co-ordinate may have a more conventional shape. Le Noble, Miller and Hamann (11) have shown that the more conventional shape shown in Fig.7 is in general represented by a quartic with two adjustable parameters:-

$$E = ax^4 + bx^3 - (2a + 1.5b)x^2 \qquad (1)$$

where the thermodynamic difference, E_1, is given at $x = 1$ by
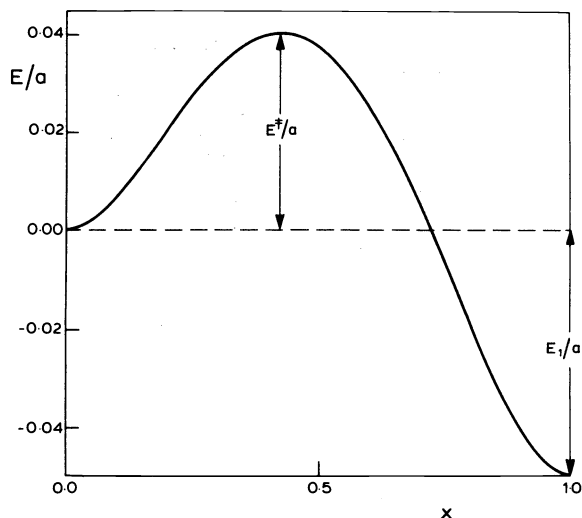
$$E_1 = -(a + \tfrac{1}{2}b)$$

Fig.7. A typical quartic energy profile given by eqn 1 where we have taken
$b/a = -1.9$. Despite the very different shaped barrier the position of the
transition state still obeys the Marcus theory.

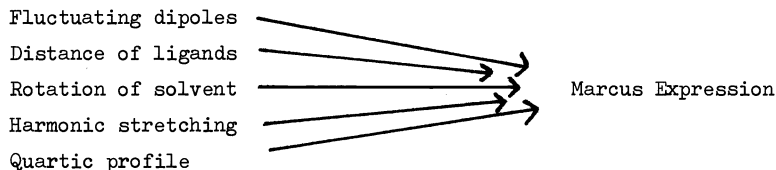Using their expression we can calculate α to be given by

$$\alpha = \tfrac{1}{2}[1 + 4y + \tfrac{1}{2}y(1 - 27y^2)] \qquad\qquad (2)$$

where $y = E_1 / 16E_{\tfrac{1}{2}}^{\ddagger} = -(1 + \tfrac{1}{2}b/a)$ and $E_{\tfrac{1}{2}}^{\ddagger}$ is the energy of activation for the symmetrical re-
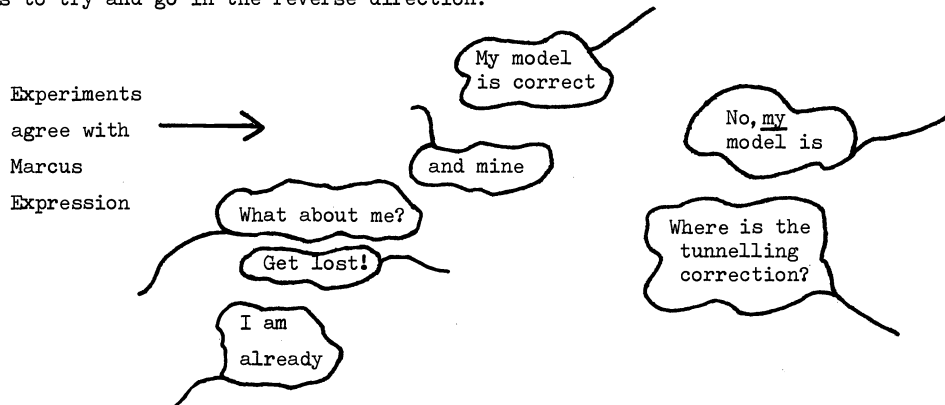action when $E_1 = 0$.

This may be compared with the expression from Marcus theory

$$\alpha = \tfrac{1}{2}(1 + 4y) \qquad\qquad (3)$$

The difference between eqn 2 and 3 is negligible being at the very most 5%. Hence the Marcus
expression is a very general one. Whatever the process required to convert a reactant into
a transition state the activation process obeys the Marcus expression. This may be sum-
marised:-

Fluctuating dipoles
Distance of ligands
Rotation of solvent   Marcus Expression
Harmonic stretching
Quartic profile

Conversely if experimental results are found to agree with the Marcus expression it is
pointless to try and go in the reverse direction:

Experiments
agree with
Marcus
Expression

My model
is correct

No, my
model is

and mine

What about me?

Where is the
tunnelling
correction?

Get lost!

I am
already

We now turn to the Marcus expression itself which can be written (12)(13) for the reaction,

$$X + CH_3Y \rightarrow XCH_3 + Y$$
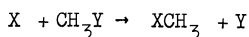
as follows:-

$$\Delta G^{\ddagger}_{X,Y} = \bar{G}_{X,Y} + \tfrac{1}{2}\Delta G^{\ominus}_{X,Y} + \frac{(\Delta G^{\ominus}_{X,Y})^2}{16(\bar{G}_{X,Y} - w^R)} \tag{4}$$

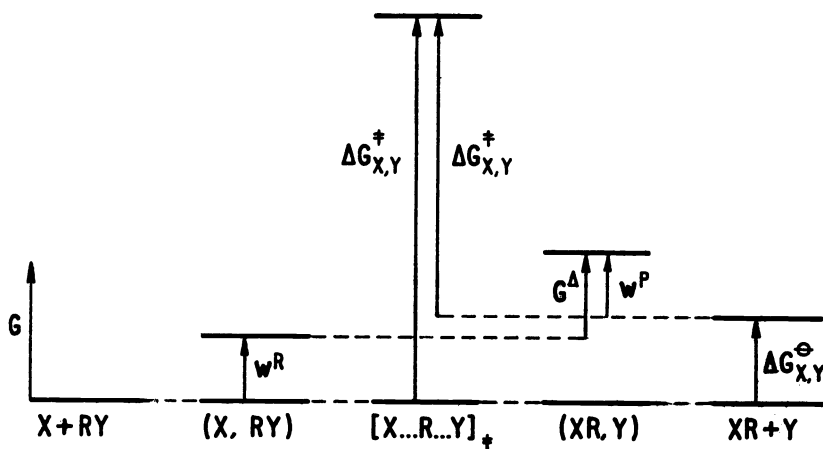where $\bar{G}_{X,Y} = \tfrac{1}{2}(\Delta G^{\ddagger}_{X,X} + \Delta G^{\ddagger}_{Y,Y})$ (5)

Fig.8. Free energy terms in the Marcus equation 4.

The free energy terms are illustrated in Fig.8. We assume throughout that $w^R = w^P = 10$ kJ mol^{-1}. For methyl transfers the w terms are small compared to $\Delta G^{\ddagger}$ terms and so our conclusions are not sensitive to this assumption. Equation 4 then gives the free energy of activation for the general (X,Y) reaction in terms of the thermodynamics, $\Delta G^{\ominus}_{X,Y}$ and the free energies of activation for the degenerate X,X and Y,Y reactions. Just as one can calculate $\tfrac{1}{2}n(n-1)$ equilibrium constants from a list of n standard electrode potentials, so, providing that the thermodynamics are known, from a list of n free energies of activation for degenerate reactions one can calculate the rate constants for n(n-1) cross reactions.

From eqn 4 we obtain the following expression for α

$$\alpha = \frac{\partial \Delta G^{\ddagger}_{X,Y}}{\partial \Delta G^{\ominus}_{X,Y}} = \tfrac{1}{2}\left[1 + \frac{\Delta G^{\ominus}_{X,Y}}{4(\bar{G} - w^R)}\right] \tag{6}$$

In investigating the properties of the transition state the absolute value of the free energy of activation is not in itself a very informative quantity. More interesting is the effect of a systematic change. For this purpose a more valuable form of eqn 4 is obtained by differentiating:-

$$d\Delta G^{\ddagger}_{X,Y} = 2\alpha(1-\alpha)[d\Delta G^{\ddagger}_{X,X} + d\Delta G^{\ddagger}_{Y,Y}] + \alpha d\Delta G^{\ominus}_{X,Y} \tag{7}$$

$$\simeq \tfrac{1}{2}[d\Delta G^{\ddagger}_{X,X} + d\Delta G^{\ddagger}_{Y,Y}] + \alpha d\Delta G^{\ominus}_{X,Y} \tag{8}$$

Figure 9 shows how the coefficients in eqn 7 vary with α. For very downhill reactions α tends to zero and the system has a neglible free energy of activation. For very uphill reactions α tends to unity; the transition state is very product-like and the free energy of activation is determined by the thermodynamic hill that has to be climbed. For fairly symmetrical reactions (0.35 < α < 0.65) the coefficient for the kinetic terms is approximately $\tfrac{1}{2}$ and we can simplify eqn 7 to give eqn 8. This approximation holds for nearly all methyl transfers.
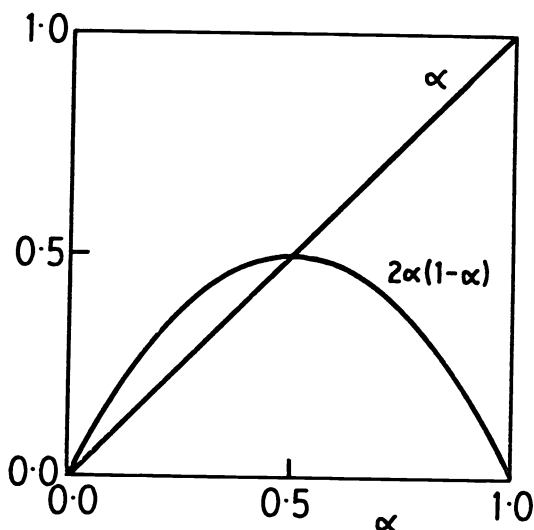
Fig.9. Plot of the coefficients in the differential form of the Marcus eqn,
eqn 7. The coefficient of the thermodynamic term, α, increases steadily as
the free energy of the transition state switches from being reactant-like
to product-like. The kinetic coefficient, $2\alpha(1-\alpha)$ is important for sym-
metrical transition states but is zero for either a very reactant-like or a
very product-like transition state; the free energies of these transition
states are respectively determined by the free energies of the reactants
and of the products.

It is important to point out that the free energy of activation has a kinetic component
given by the terms in $\Delta G^{\ddagger}_{X,X}$ and $\Delta G^{\ddagger}_{Y,Y}$ as well as a thermodynamic component given by the term
in $\Delta G^{\ominus}_{X,Y}$. For proton transfers, where a series of catalysts, HA, are used, because $d\Delta G^{\ddagger}_{A^-,A}$
is very small, eqn 7 simplifies to

$$d\Delta G^{\ddagger}_{A^-,Y} \simeq \alpha d\Delta G^{\ominus}_{A^-,Y} \qquad\qquad (9)$$

This equation is the basis of the Brønsted-Marcus relation. However this simplification
only applies to proton transfers. For methyl transfers changing the nucleophile X changes
$\Delta G^{\ddagger}_{X,Y}$ not only through the thermodynamic term but also through $\Delta G^{\ddagger}_{X,X}$.

APPLICATION TO METHYL TRANSFERS

Returning to eqn 4 for any methyl transfer,

$$X + CH_3Y \rightarrow XCH_3 + Y,$$
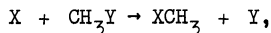
given a value of the free energy of activation $\Delta G^{\ddagger}_{X,Y}$, we can calculate $\bar{G}_{X,Y}$ the kinetic
term, providing that the thermodynamic term $\Delta G^{\ominus}_{X,Y}$ is known. The values of $\Delta G^{\ominus}_{X,Y}$ have
been calculated from tables published by Abraham and McLennan (14) supplemented by some extra
values calculated by Abraham (15). The kinetic term (eqn 5) is the sum of two contributions
from the degenerate X and Y reactions. If we have two different nucleophiles X_1 and X_2
reacting with a series of different leaving groups, Y_n, then if the Marcus pattern is
correct eqn 10 should hold:-

$$\Delta\bar{G} = \bar{G}_{X_1,Y} - \bar{G}_{X_2,Y} = \tfrac{1}{2}(\Delta G^{\ddagger}_{X_1,X_1} - \Delta G^{\ddagger}_{X_2,X_2}) \quad = \text{a constant} \qquad (10)$$

Typical results are given in Table 1. It can be seen that $\Delta\bar{G}$ is approximately constant. We
can then calculate (13) the values for $\Delta G^{\ddagger}_{X,X}$ given in Table 2. We find that I^- has the
lowest barrier. There is a steady increase in the series I^- through to F^-. All the
oxygen compounds, except for NO_3^- and OH^-, have barriers of about 150 kJ mol^{-1}. There may
be an extra desolvation term for OH^- in that replacing a water molecule with the substrate
may be particularly difficult for this species. We have therefore repeated the calculation
for OH_* in which the barrier is divided into a 'normal' oxygen barrier of 147 kJ mol^{-1} and
an extra desolvation term of 20 kJ mol^{-1}. Finally CN^- has the largest barrier. No doubt
this is because the making and breaking of C-C bonds requires more energy than for the other
species.

TABLE 1.   Test of Eqn 10 for OH^- and I^-

Y	$\bar{G}_{OH^-,Y}$	$\bar{G}_{I^-,Y}$	$\Delta\bar{G}$
	$\overline{\text{kJ mol}^{-1}}$	$\overline{\text{kJ mol}^{-1}}$	$\overline{\text{kJ mol}^{-1}}$
φSO_3^-	160	125	35
NO_3^-	145	103	42
F^-	152	119	33
Cl^-	145	101	44
Br^-	140	95	45
I^-	138	92	46

TABLE 2.   Values of $\Delta G_{X,X}^{\ddagger}$ for degenerate methyl transfers in H_2O at $25^{\circ}C$

X	X	$\Delta G_{X,X}^{\ddagger}/\text{kJ mol}^{-1}$
I^-	I^-	97
Br^-	Br^-	99
Cl^-	Cl^-	111
NO_3^-	NO_3^-	111
F^-	F^-	133
OTs^-	OTs^-	145
$CH_3SO_3^-$	$CH_3SO_3^-$	145
H_2O	H_2O	147
φSO_3^-	φSO_3^-	149
$CH_3OSO_3^-$	$CH_3OSO_3^-$	150
ClO_4^-	ClO_4^-	155
OH_*^- [a]	OH_*^- [a]	167
OH^-	OH^-	175
CN^-	CN^-	213

[a] OH_*^- calculated with 20 kJ mol^{-1} extra desolvation (167 = 20 + 147)

In Fig.10 we compare the values of $\bar{G}_{X,Y}$ calculated from $\Delta G_{X,Y}^{\ddagger}$ and $\Delta G_{X,Y}^{\ominus}$ and eqn 4, with those calculated from the $\bar{G}_{X,X}$ values using eqn 5 and Table 2.

The good straight line of unit slope shows the success of the treatment and confirms the earlier work of German and Dogonadse (16)(17). It is worth pointing out that the data in Table 2 (together with the corresponding thermodynamic data) already allow one to calculate the free energies of activation for 156 different reactions.

Once the Marcus pattern is established we can now proceed to calculate values of α for the different reactions. The results are given in Table 3. It can be seen that for nearly all these reactions α is fairly close to 0.5. This is because for methyl transfers the kinetic barriers are quite large and therefore α is relatively insensitive to imbalance in the thermodynamics. It also means that the approximation in going from eqn 7 to eqn 8 is justified for methyl transfers.

Other solvents   Using the transfer activity coefficients calculated by Parker and co-workers (18) we can extend the analysis to methanol and dimethylformamide. We can also calculate $\Delta G_{X,X}^{\ddagger}$ for reactions in acetone from the data obtained by Moelwyn Hughes and his collaborators (19). In each solvent the Marcus pattern is again found (13). The results for $\Delta G_{X,X}^{\ddagger}$ for the halide reactions are displayed in Fig.11. For each solvent the barrier for I^- is less than that for Br^- which in turn is less than that for Cl^-. For each ion the barrier decreases as the solvent changes from a hydroxylic solvent (H_2O or MeOH) for the less polar solvent (dimethylformamide or acetone). This pattern is exactly what one would expect if part of the free energy of activation is concerned with reorganizing the solvent around the X,X pair. Remember that all these reactions are degenerate. The barriers in Fig.11 are purely kinetic and the analysis has removed the effect of the thermodynamics.
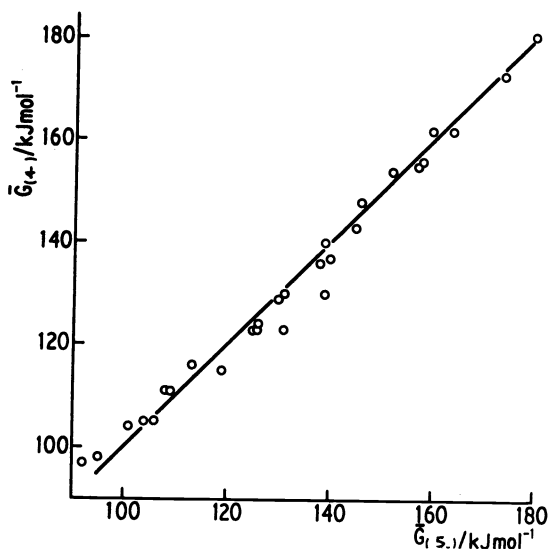
Fig.10. Test of the Marcus theory for methyl transfers in H_2O. The graph compares the values of $\bar{G}_{X,Y}$ calculated from $\Delta G_{X,Y}^{\ddagger}$, $\Delta G_{X,Y}^{\ominus}$ and eqn 4 ($\bar{G}_{(4)}$) with those calculated from eqn 5 and the values in Table 2 for the degenerate reactions ($\bar{G}_{(5)}$).

TABLE 3.   Values of α

Nucleophile X						
NO_3^-	0.43	0.50				
Cl^-	0.43	0.50	0.50	0.50		
Br^-	0.43	0.51	0.50	0.51	0.50	
I^-	0.42	0.50	0.49	0.50	0.49	0.50
H_2O	0.43	0.50	0.49	0.49	0.49	0.50
CN^-	0.34	-	0.38	0.38	0.37	0.38
OH^-	0.37	0.42	0.42	0.41	0.41	0.41
OH_*^-	0.33	0.39	0.39	0.38	0.37	0.38
Leaving Group						
Y	φSO_3^-	NO_3^-	F^-	Cl^-	Br^-	I^-

SWAIN SCOTT RELATION

The simplest measure of nucleophilic activity that has been used hitherto is the Swain Scott relation (20). In our notation the relation is:-

$$\log k_{X,Y} = \log k_{H_2O,Y} + s_Y n_X \qquad (11)$$

where
$$n_X = \log k_{X,Br^-} - \log k_{H_2O,Br^-}$$
$$= \frac{\Delta G_{H_2O,Br^-}^{\ddagger} - \Delta G_{X,Br^-}^{\ddagger}}{2.3\ RT}$$

From the Marcus treatment we can now separate n_X into a kinetic and a thermodynamic contribution:-

$$n_X = n_X^{\ddagger} + n_X^{\ominus} \qquad (12)$$

where
$$n_X^{\ddagger} = \frac{\Delta G_{H_2O,H_2O}^{\ddagger} - \Delta G_{X,X}^{\ddagger}}{4.6\ RT} \qquad (13)$$
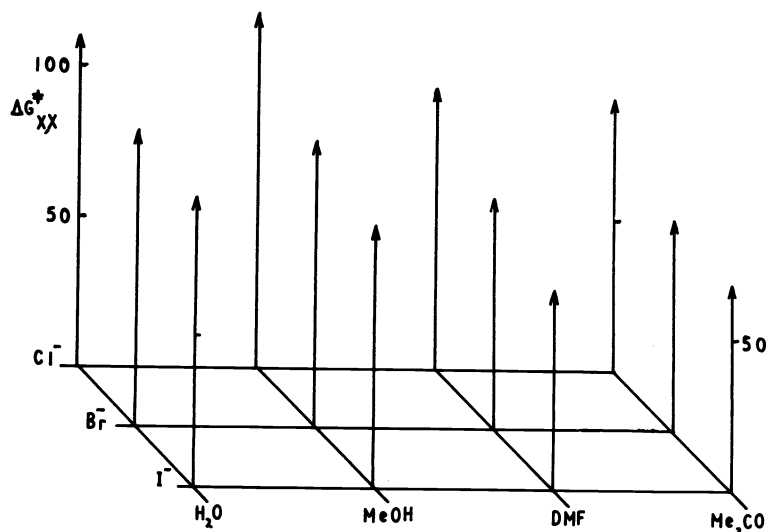
Fig.11. Free energies of activation (in kJ mol^{-1}) for the degenerate re-
actions of Cl$^-$, Br$^-$ and I$^-$ in H$_2$O, MeOH, dimethyl formamide (DMF) and
acetone.

$$\text{and } n_X^{\ominus} \simeq \frac{\Delta G_{H_2O,X}^{\ominus}(\alpha_{X,Br^-} + \tfrac{1}{2})}{4.6 \; RT} \tag{14}$$

The results of this analysis are shown in Fig.12. Each nucleophile is compared with water.
It can be seen that the balance of the kinetic and thermodynamic terms in eqn 12 can be very
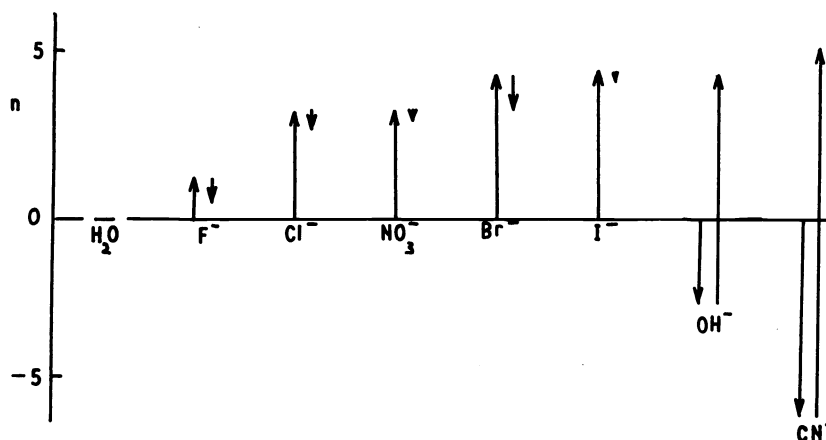different. For instance I$^-$ is a good 'kinetic' nucleophile compared to water, because, as

Fig.12. Kinetic and thermodynamic contributions to the Swain Scott nucleo-
philicity parameter, n; calculated from eqn 12 to 14. The left hand arrow
of each pair shows the kinetic contribution.

discussed above, $\Delta G_{I^-,I^-}^{\ddagger}$ is much less than $\Delta G_{H_2O,H_2O}^{\ddagger}$; the thermodynamics are roughly in
balance. By contrast CN$^-$ is very poor kinetically because of the large $\Delta G_{CN^-,CN^-}^{\ddagger}$; it is the
thermodynamic driving force that makes it a good nucleophile overall. As leaving
groups, I$^-$ with its low barrier is a 'good' leaving group. On the other hand for CN$^-$ the
thermodynamics are now reversed and so both terms add together to make it a very poor leaving
group indeed. One can calculate that the half life for the hydrolysis of acetonitrile is
10^{-28} years.

A similar problem arises with s_Y in eqn 11. From eqn 7 and Fig.9 the coefficients are not the same for the kinetic and thermodynamic contributions. If changing the nucleophile, X, mainly changes the kinetic contribution $n_X^{\ddagger}$ then

$$s_Y^{\ddagger} \simeq 4\,\alpha_{X,Y}\,(1 - \alpha_{X,Y}) \tag{28}$$

On the other hand if changing the nucleophile mainly changes the thermodynamic contribution then

$$s_Y^{\ominus} = 2\alpha_{X,Y} \tag{16}$$

As shown in Fig.9 for $\alpha_{X,Y} \simeq \frac{1}{2}$ we find that $s_Y^{\ddagger} \simeq s_Y^{\ominus} \simeq 1.0$. This of course holds for the hydrolysis of methyl bromide. However in general because of the mix of kinetic and thermodynamic contributions we cannot expect a simple linear free energy relation of the Swain Scott type to hold for all reactions and all nucleophiles. This has indeed been found to be the case (21)(22) and more complicated relations such as the Edwards relation (23) have been suggested. It is however worth pointing out that for the halide ions (and H_2O) the main contribution to n is the kinetic term. Hence for this restricted group of nucleophiles, we may expect that the simple LFER may hold and we may use eqn 15 to calculate $\alpha_{X,Y}$ from s_Y. For instance for the displacement of N_2 from diazonium ions, where $s \sim 0.4$ (24)(25), we find $\alpha \sim 0.1$. This result also agrees with the solvent isotope effect for the reaction (26)(27). The nucleophilic involvement is very weak because N_2 is such a good thermodynamic leaving group.

THE MEASUREMENT OF CHARGE DEVELOPMENT

Having discussed the Marcus theory, we now turn to other probes of transition state structure. For ionogenic reactions Abraham (28) has tried to measure the development of charge in the transition state from the variation of the reaction rate on changing the solvent from water to methanol. In the reaction

$$X + RY \rightarrow [\overset{\delta+}{X} \ldots R \ldots \overset{\delta-}{Y}]_{\ddagger} \rightarrow (XR^{+},Y^{-})$$
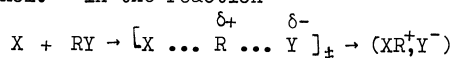
the free energy of transferring the species from water to methanol ($\Delta G^{H_2O,MeOH}$) is separated into two contributions concerned firstly with the volume of the solute (or transition state) and secondly with the electrostatic contribution ($\Delta G_e^{H_2O,MeOH}$). The volume contribution is estimated using 11 non-polar species such as noble gases. The separation was tested using 12 different ion pairs of the type (R_4N^{+},Y^{-}) and Abraham found (28) that despite their different sizes the electrostatic contribution was reasonably constant:-

$$\Delta G_e^{H_2O,MeOH} = (31 \pm 3)\ kJ\ mol^{-1}$$

This is therefore the limiting value for the complete development of the ion pair and Abraham then measures the charge development with the parameter Z:-

$$Z = \frac{\Delta G_{e,\ddagger}^{H_2O,MeOH}}{\Delta G_{e,(R_4N^{+},Y^{-})}^{H_2O,MeOH}} \tag{15}$$

Values of Z are collected together in Table 4. We also report values of $\sqrt{Z}$. The reason for this is that the free energy for transferring a dipole of moment μ has been shown to be

TABLE 4. Values of charge development parameter, Z

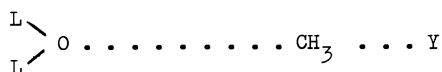| X	R	Y	Z	$\sqrt{Z}$
S [a]	Me	Br	0.28	0.53
S [a]	Me	I	0.31	0.56
Me_3N	Me	I	0.42	0.65
Et_3N	Et	I	0.45	0.67
—	tBu	Cl	0.85	0.92

[a] S is the Solvent

proportional to μ^2 (29). Hence if the bond order, n_Y, is related to the development of the dipole moment, we obtain,

$$1 - n_Y = \mu_{\ddagger}/\mu_{R_4N^{+}Y^{-}} = \sqrt{Z} \tag{16}$$

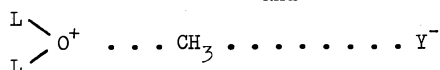Further discussion of Z and $\sqrt{Z}$ values is deferred until the other probes have been examined.

SOLVENT ISOTOPE EFFECT

Whereas the charge development measures η_Y, the bond order of the leaving group, the solvent isotope effect should measure η_X, the bond order of the incoming L_2O molecule where L represents either H or D.   By analogy with the Gold-Kresge relation (30)(31) for proton transfer we can expect that the fractionation factor, $\varphi_\ddagger$, for the incoming nucleophile will lie between two extremes:-

$$\begin{array}{l} L \\ \diagdown \\ O \cdot \cdot \cdot \cdot \cdot \cdot \cdot \cdot \cdot \cdot CH_3 \cdot \cdot \cdot Y \\ \diagup \\ L \end{array}$$

$\varphi_\ddagger \simeq 1$

and

$$\begin{array}{l} L \\ \diagdown \\ O^+ \cdot \cdot \cdot CH_3 \cdot \cdot \cdot \cdot \cdot \cdot \cdot \cdot Y^- \\ \diagup \\ L \end{array}$$

$\varphi_\ddagger \simeq \varphi_L$

where φ_L is the limiting value for $L_2O^+CH_3$.   It is probable that φ_L lies between the value of 0.69 for L_3O^+ in L_2O (32)(33) and the value of 0.63 for $L_2O^+CH_3$ in CH_3OL (34).   The equivalent of the Gold-Kresge relation is

$$\varphi_\ddagger = \varphi_L{}^{\eta_X} \tag{17}$$

By the usual Kresge treatment (31) the observed solvent isotope effect is given by

$$k_{D_2O}/k_{H_2O} = (\varphi_\ddagger)^2 \; \Phi_Y \tag{18}$$

where Φ_Y describes the fractionation around the leaving group (35), rather than the incoming nucleophile.

We have attempted to separate the contributions from $\varphi_\ddagger$ and Φ_Y for the hydrolysis of methyl bromide by using a differential conductivity method and studying the reaction in 50% D_2O as well as 100% D_2O.   We found (27)

$$\varphi_\ddagger = 0.92 \pm 0.02$$

and $\Phi_{Br} = 0.95 \pm 0.04$.

These results suggest that the main contribution is from the L_2O nucleophile rather than the leaving group.

We also reach the same conclusion by comparing the solvent isotope effects for Cl^- and Br^- as leaving groups.   For the fully developed anions Salomaa (36)(37) has shown that

$$\Phi_{Cl^-} / \Phi_{Br^-} = 1.15$$

If Φ_Y is important in S_N2 solvent isotope effects then we would expect that there would be a systematic difference between Cl^- and Br^- as leaving groups.   Using the data of Laughton and Robertson (38), and, after correcting for the different temperatures at which the isotope effects were measured, we obtain the results in Table 5.

TABLE 5.   Solvent isotope effects for S_N2 reactions involving Cl^- and Br^-

R	$\dfrac{T_{Br}}{°C}$ [a]	$\dfrac{T_{Cl} - T_{Br}}{°C}$ [b]	$\left(\dfrac{k_{D_2O}}{k_{H_2O}}\right)_{Cl}$	$\left(\dfrac{k_{D_2O}}{k_{H_2O}}\right)_{Br}$	Ratio
Et	100	0	0.81	0.82	0.99
Me	70	20	0.77	0.79	0.98
$CH_2 = CHCH_2$	60	15	0.78	0.77	1.01
C_6H_{11}	60	0	0.77	0.77	0.99
$PhCH_2$	30	30	0.77	0.74	1.04
$pMeC_6H_4CH_2$	20	10	0.74	0.745	<u>0.99</u>
				Mean	1.00

[a] Temperature at which solvent isotope effect for RBr was measured.

[b] Temperature range over which result for RCl had to be corrected by
$$T_2 \; ln \, (k_{D_2O}/k_{H_2O})_{T_2} = T_1 \; ln \, (k_{D_2O}/k_{H_2O})_{T_1}$$

It can be seen that there is no systematic difference. Hence while for S_N1 reactions the solvent isotope effect must be caused by Φ_Y, we conclude that for S_N2 reactions the main contribution is that from $\varphi_{\ddagger}$ and we put $\Phi_Y = 1$. Then for the hydrolysis of methyl bromide after correcting to 298 K we find from eqn 17 and 18:-

$$\eta_X = 0.33 \quad \text{for} \quad \varphi_L = 0.63 \tag{19}$$

$$\text{or} \quad \eta_X = 0.41 \quad \text{for} \quad \varphi_L = 0.69 \tag{20}$$

α DEUTERIUM ISOTOPE EFFECTS

The substitution of D for H on the transferring methyl group is a small enough change for us to use the differential form of the Marcus equation as given in eqn 8. For many reactions the isotope substitution has very little effect on the thermodynamics and so,

$$\frac{dG^{\ddagger}_{X,Y}}{dI} \simeq \frac{1}{2}\left[\frac{dG^{\ddagger}_{X,X}}{dI} + \frac{dG^{\ddagger}_{Y,Y}}{dI}\right] \tag{21}$$

This relation also holds exactly when $\alpha = \frac{1}{2}$. In terms of fractionation factors for the transition state we find

$$\varphi^{\ddagger}_{X,Y} = (\varphi^{\ddagger}_{X,X} \varphi^{\ddagger}_{Y,Y})^{\frac{1}{2}} \tag{22}$$

Again we have a pattern in which the isotope effect for the cross reaction is a simple fraction of the isotope effects for the two degenerate reactions. There are sufficient data to test eqn 22 as shown in Table 6. From eqn 22,

$$\Delta = \log \varphi^{\ddagger}_{X_1,Y} - \log \varphi^{\ddagger}_{X_2,Y} = \frac{1}{2}\log(\varphi^{\ddagger}_{X_1,X_1}/\varphi^{\ddagger}_{X_2,X_2})$$

TABLE 6 Test of Marcus Pattern for α-deuterium isotope effects

Y	X_1	X_2	$\log \varphi^{\ddagger a}_{X_1,Y}$	$\log \varphi^{\ddagger a}_{X_2,Y}$	Δ
$CH_3SO_3^-$	H_2O	$S_2O_3^=$	0.042	0.024	0.018
Br^-	H_2O	$S_2O_3^=$	0.017	0.004	0.013
I^-	H_2O	$S_2O_3^=$	0.009	-0.010	0.019

a The fractionation factors are measured with respect to the standard reaction $MeCH_2D + X...CH_3..Y \rightleftharpoons MeCH_3 + X...CH_2D..Y$

The quantity Δ is reasonably constant and independent of Y. From the compilations of Shiner (39) and of Robertson et al. (40) we then obtain the results given in Table 7.

TABLE 7 α-Deuterium isotope effects for degenerate reactions

X	φ_{RX}	$\varphi^{\ddagger}_{X,X}$	$(k_D/k_H)^{\frac{1}{3}} = \varphi^{\ddagger}_{X,X}/\varphi_{RX}$
I^-	0.967	0.936	0.968
Br^-	0.998	0.970	0.972
$CH_3OSO_3^-$	1.078	1.059	0.982
Cl^-	1.033	1.024	0.991
NO_3^-	1.078	1.083	1.005
$CH_3SO_3^-$	1.078	1.087	1.008
CH_3COO^-	1.078	1.087	1.008
ClO_4^-	1.078	1.100	1.020
$S_2O_3^=$	0.998	1.019	1.021
H_2O	1.078	1.115	1.034
CN^-	1.009	1.050	1.040

Comparison of the results in Table 3 with those in Table 7 shows that the same order, I^-, Br^-, Cl^-, $-O^-$, CN^- is found in both Tables. The degenerate reaction for I^- has a low barrier and a low α-deuterium isotope effect, as opposed to CN^- which has a high barrier and a high isotope effect. The two sets of data and the two analyses are quite separate and are only linked through the application of the Marcus expression. The agreement therefore provides further confirmation of the Marcus pattern. Shiner has shown (41) that the α-deuterium

factor, φ_+, for the carbonium ion is $\varphi_+ \simeq 0.81$.   Hence a low α-deuterium isotope effect suggests carbonium ion character.   Remembering that all these reactions in Table 7 are degenerate and must have $\alpha = \frac{1}{2}$ we suggest that the variation in the α-deuterium isotope effect is caused by a variation in the tightness or bond order of the transition state. We write (13)

$$\tau_{X,X} \simeq \frac{\varphi^{\ddagger}_{X,X} - \varphi_+}{\varphi_{RX} - \varphi_+}$$

If $\varphi^{\ddagger}_{X,X} = \varphi_+$ then $\tau_{X,X} = 0$ and the system passes through the carbonium ion corner.   On the other hand if $\varphi^{\ddagger}_{X,X} = \varphi_{RX}$ then the observed isotope effect is unity, $\tau = 1$, and the system preserves its bond order throughout.   Using eqn 23 we can now plot the results from Tables 3 and 7 on the same diagram in Fig.13.   The stronger the bond to be broken (e.g. CN^-), the higher the barrier, and the tighter the transition state has to be.   On the other hand if the bonds are weak (e.g. I^-) then there does not have to be so much 'involvement' and the repulsive forces keep the transition state loose.   Again the advantage of the Marcus analysis is that it allows us to separate out the effects of the thermodynamics.   It is easier to discuss the pattern of reactivity for degenerate reactions lined up on $\alpha = \frac{1}{2}$.
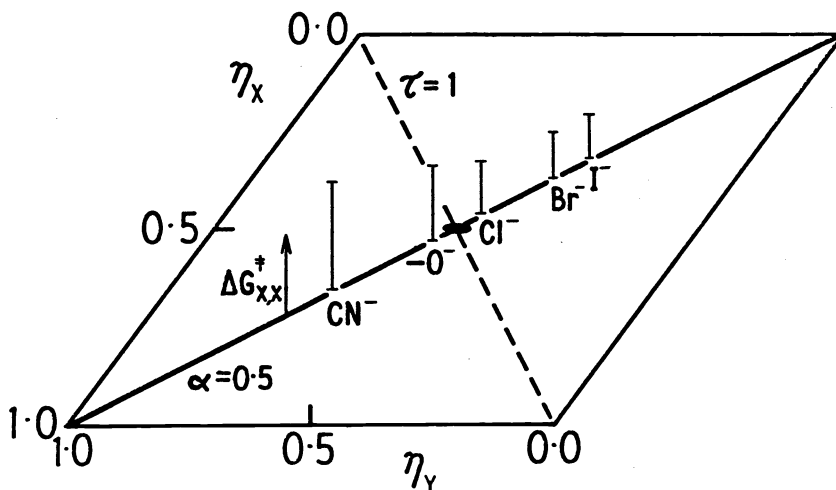

Fig.13. The location of the transition states for degenerate reactions in H_2O.   The values of τ are calculated from the α-D isotope effect (Table 7). The free energies of activation (Table 2) are shown by the vertical lines.

HAMMETT RELATIONS

When the attacking nucleophile or the leaving group is aromatic then more information about the transition state can be found by the use of substituents and application of the Hammett $\sigma\rho$ relation.   From eqn 8 we find for a linear free energy relation that

$$\rho_{X,Y} = \frac{1}{2}\rho^{\ddagger}_{X,X} + \frac{1}{2}\rho^{\ddagger}_{Y,Y} + \alpha\rho^{\ominus}_{X,Y}$$

For substitution on an attacking nucleophile, X, with the same leaving group Y $\rho^{\ddagger}_{Y,Y} = 0$. Then assuming $\alpha \simeq \frac{1}{2}$ we find
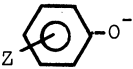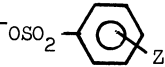
$$\rho^{\ddagger}_{X,X} = 2\rho_{X,Y} - \rho^{\ominus}_{X,Y} \qquad\qquad (24)$$

Similarly for substitution on the leaving group for the same attacking nucleophile we find

$$\rho^{\ddagger}_{Y,Y} = 2\rho_{X,Y} - \rho^{\ominus}_{X,Y} \qquad\qquad (25)$$

In order to separate the kinetics and thermodynamics we need to know $\rho^{\ominus}_{X,Y}$.   For attack by substituted phenolate ions we use ρ for the ionisation of the phenols (42).   For the solvolysis reactions we use ρ for the solvolysis of the corresponding adamantyl compounds (43), on the grounds that the transition state is very product-like, and the full difference caused by the substitution in the leaving group is therefore observed.   Results for several systems (44) are collated in Table 8.   From the values for $\rho^{\ominus}_{X,Y}$ we can see that the limiting value for the carbonium ion corner will be $\rho \simeq 2$.   The sign is of course different depending on

TABLE 8   Results for $\rho^{\ddagger}_{X,X}$ or $\rho^{\ddagger}_{Y,Y}$

X	Y	$\rho_{X,Y}$	$\rho^{\ominus}_{X,Y}$	$\rho^{\ddagger}_{X,X} = \rho^{\ddagger}_{Y,Y}$
Z⟨benzene⟩-O⁻	$CH_3OSO_3^-$	-0.81	-2.1	0.5
Z⟨benzene⟩-O⁻	I⁻	-0.99	-2.4	0.4
Solvent	⁻OSO₂-⟨benzene⟩Z	1.3	1.8	0.8

whether the substitution is on X or Y.   It is satisfactory that the values found for $\rho^{\ddagger}_{X,Y}$ are in rough agreement and are considerably less than the limiting value.   We might expect that $\rho_{X,Y} \simeq 0$ for the $\tau = 1$ line.   This is because, if the bond order is preserved in the degenerate transition state, then, taking Z to be more electron withdrawing, one should have perfect compensation between the poorer nucleophile and the better leaving group. If this argument is correct, then the results in Table 8 suggest that the transition states for these reactions are slightly 'loose'.   Once again we must emphasise how important it is to separate $\rho_{X,Y}$ into its thermodynamic and kinetic contributions.

FINAL DISCUSSION

We now collect together the information about the location of the transition state obtained from the different probes.   We start by considering the hydrolysis of methyl bromide since we have the most data for this reaction.   The results may be summarised (see Fig.14):-

1) Marcus analysis $\alpha = 0.5$

2) Abraham Z parameter $\eta_Y = 1 - Z = 0.72$
                                    or $\eta_Y = 1 - Z^{\frac{1}{2}} = 0.44$

3) Solvent isotope effect $\varphi_L = 0.63$ gives $\eta_X = 0.33$
                                    $\varphi_L = 0.69$ gives $\eta_X = 0.41$

4) α-Deuterium isotope effect $\tau \simeq 1.0$

5) Hammett relation $\tau \simeq 0.7$ to 0.8
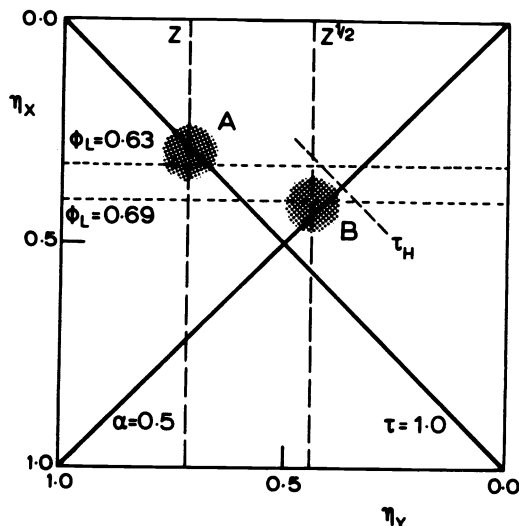

Fig.14. The location of the transition state for the hydrolysis of MeBr. The full lines show the values of α and τ from the Marcus analysis and the α-D isotope effect respectively.   The broken lines show the values of η_Y from the charge development parameter Z.   The dotted lines show the values of η_X from the solvent isotope effect.   The line labelled τ_H is an indication from the analysis of the Hammett ρ.   Previous arguments placed the transition state at A. The Marcus analysis suggests that B is more probable.

Previous analysis based on the Abraham Z parameter (using Z) (28) on the solvent isotope effect (45) and on the α-deuterium isotope effect has placed the transition state for this reaction somewhere around A.   That is an early transition state with α ~ 0.3.   We believe that the Marcus analysis rules out this possibility and that the transition state must be in the shaded area B.   This transition state is reasonably consistent with all the different probes.   It suggests that one should use $\sqrt{Z}$ to find η_Y from the Abraham Z parameter and $\varphi_L = 0.69$ for interpretation of the solvent isotope effect.

For other reactions, if they are degenerate, then the pattern presented in Fig.13 shows the location of the transition state.   For cross reactions the tightness, τ, will be intermediate between the values for the degenerate reactions:-

$$\tau_{X,Y} \simeq \tfrac{1}{2}(\tau_{X,X} + \tau_{Y,Y})$$

The value of α can be calculated for the Marcus expression; many values are given in Table 3. Knowing τ and α the transition state can then be located on the map.

Finally we summarise the main conclusions

1) The Marcus expression holds for methyl transfers.

2) The analysis from the Marcus expression allows one to separate observed $\Delta G^{\ddagger}$, isotope effects or linear free energy parameters into kinetic and thermodynamic contributions.

3) It is much easier to consider variations in the free energies of activation of degenerate reactions where the thermodynamic contribution is zero.

4) Transition states should be located with respect to τ as well as α.   For this purpose Albery-More O'Ferrall diagrams are useful.

5) For methyl transfer reactions there is a greater variation in τ rather than in α.

6) The higher the barrier for a degenerate reaction, the tighter is the transition state and the larger is the α-deuterium isotope effect.

7) For the same degenerate reaction a change of solvent from a hydroxylic solvent to a less polar non-hydroxylic solvent lowers the barrier and tightens the transition state.

This work arose out of collaboration with Professor Maurice Kreevoy when he was on sabbatical leave in Oxford; I am more than usually grateful to him for formative and informative discussions.

REFERENCES

1.   R. A. Marcus, J. Phys. Chem. 67, 853-857 (1963).
2.   R. A. Marcus, Ann. Rev. Phys. Chem. 15, 155-196 (1964).
3.   R. A. Marcus, Electrochim. Acta, 13, 995-1004 (1968).
4.   R. A. Marcus, J. Phys. Chem. 72, 891-899 (1968).
5.   R. A. Marcus, Faraday Symp. 10, 60-68 (1975).
6.   W. J. Albery, Prog. Reaction Kinetics, 4, 353-398 (1967).
7.   R. A. More O'Ferrall, J. Chem. Soc. (B), 274-277 (1970).
8.   W. P. Jencks, Chem. Rev. 705-718 (1972).
9.   V. Gold, J. Chem. Soc. 4633-4637 (1956).
10. W. J. Albery, Electrode Kinetics, Clarendon Press, Oxford, p.105 (1975).
11. W. J. Le Noble, A. R. Miller and S. D. Hamann, J. Org. Chem. 338-342 (1977).
12. W. J. Albery, Electrode Kinetics, Clarendon Press, Oxford, p.121 (1975).
13. W. J. Albery and M. M. Kreevoy, Adv. Phys. Org. Chem. to be published.
14. M. H. Abraham and D. J. McLennan, J.C.S. Perkin II, 873-879 (1977).
15. M. H. Abraham, personal communication.
16. E. D. German and R. R. Dogonadse, Int. J. Chem. Kinetics, 6, 457-466 (1974).
17. E. D. German and R. R. Dogonadse, Int. J. Chem. Kinetics, 6, 467-479 (1974).
18. R. Alexander, E. C. F. Ko, A. J. Parker and T. J. Broxton, J. Amer. Chem. Soc. 90, 5049-5069 (1968).
19. E. A. Moelwyn-Hughes, The Chemical Statics and Kinetics of Solution, Academic Press, London, 219-227 (1971).
20. C. G. Swain and C. B. Scott, J. Amer. Chem. Soc. 75, 141-147 (1953).
21. J. E. Leffler and E. Grunwald, Rates and Equilibria of Organic Reactions, Wiley, New York, 246-254 (1963).
22. J. Koskikallio, Acta Chem. Scand. 26, 1201-1208 (1972).
23. J. E. Edwards, J. Amer. Chem. Soc. 76, 1540-1547 (1954).
24. C. E. McCauley and C. V. King, J. Amer. Chem. Soc. 74, 6221-6232 (1952).
25. W. J. Albery, J. E. C. Hutchins, R. M. Hyde and R. H. Johnson, J. Chem. Soc. B, 219-224 (1968).
26. W. J. Albery and M. H. Davies, Trans. Faraday Soc. 65, 1066-1073 (1969).

27. W. J. Albery and J. S. Curran, Finnish Chem. Lett. 3-6 (1978).
28. M. H. Abraham, Prog. Phys. Org. Chem. 11, 1-87 (1974).
29. J. G. Kirkwood, J. Chem. Phys. 2, 351-361 (1934).
30. V. Gold, Trans. Faraday Soc. 56, 255-261 (1960).
31. A. J. Kresge, Pure Appl. Chem. 8, 243-258 (1964).
32. V. Gold, Proc. Chem. Soc. 141-143 (1963).
33. A. J. Kresge and A. L. Allred, J. Amer. Chem. Soc. 85, 1541-1541 (1963).
34. V. Gold and S. Grist, Chem. Comm. 1216-1217 (1968)
35. W. J. Albery, Proton Transfer Reactions (E. F. Caldin and V. Gold, eds.), Chapman and Hall, London, 271-272 (1975).
36. P. Salomaa, Acta Chem. Scand. 25, 365-373 (1971).
37. W. J. Albery, Proton Transfer Reactions (E. F. Caldin and V. Gold, eds.), Chapman and Hall, London, p.283 (1975).
38. P. M. Laughton and R. E. Robertson, Can. J. Chem. 37, 1491-1497 (1959).
39. V. J. Shiner, Isotope Effects in Chemical Reactions (C. J. Collins and N. S. Bowman, eds) Rheinhold, New York, p.98 (1971).
40. R. E. Robertson, A. Annesa and J. M. W. Scott, Can. J. Chem. 53, 3106-3115 (1975).
41. V. J. Shiner, Isotope Effects in Chemical Reactions (C. J. Collins and N. S. Bowman, eds) Rheinhold, New York, p.107 (1971).
42. C. M. Judson and M. Kilpatrick, J. Amer. Chem. Soc. 71, 3115-3120 (1949).
43. D. N. Kevill, C. J. Kolwyck, D. M. Shold and C. Kim, J. Amer. Chem. Soc. 95, 6022-6027 (1973).
44. H. H. Jaffé, Chem. Rev. 53, 191-261 (1953).
45. R. L. Schowen, Prog. Phys. Org. Chem. 9, 273-332 (1972).